

Bottomed baryon decays with invisible Majorana fermions

Geng Li^a, Chia-Wei Liu, Chao-Qiang Geng

*School of Fundamental Physics and Mathematical Sciences,
Hangzhou Institute for Advanced Study, UCAS, 310024 Hangzhou, China
University of Chinese Academy of Sciences, 100190 Beijing, China*

Abstract

We study the invisible Majorana fermions of χ in bottomed baryon decays with flavor-changing neutral currents (FCNCs) based on the model-independent effective Lagrangian between the quarks and invisible particles. From the bounds of the coupling constants extracted from the experiments, we examine the decay branching ratios of $\Lambda_b \rightarrow \Lambda\chi\chi$, $\Xi_b^{0(-)} \rightarrow \Xi^{0(-)}\chi\chi$, $\Lambda_b \rightarrow n\chi\chi$, $\Xi_b^- \rightarrow \Sigma^-\chi\chi$, $\Xi_b^0 \rightarrow \Sigma^0\chi\chi$, and $\Xi_b^0 \rightarrow \Lambda\chi\chi$, which can be as large as 6.3, 9.2, 5.7, 5.8, 2.7, and 1.0×10^{-5} for $m_\chi = 2$ GeV, respectively. Some of these decays are accessible to the future experimental searches, such as Belle II.

^a ligeng@ucas.ac.cn

I. INTRODUCTION

It is known that flavor-changing neutral current (FCNC) processes of long-lived particles would provide a window to observe new physics (NP) beyond the standard model (SM). These particles, such as ground-state mesons of K , B , D , and B_c , and baryons of $\Lambda_{c,b}$ and $\Xi_{c,b}$, decay through weak interactions, resulting in longer lifetimes and narrower decay widths. These FCNC decays may benefit the detections of NP. Hadronic FCNC decays include $c \rightarrow u$, $s \rightarrow d$, $b \rightarrow d$, and $b \rightarrow s$ processes at quark level. In the SM, dilepton FCNC modes have been widely studied theoretically [1–5] and experimentally [6–10]. However, the neutrino (ν) and anti-neutrino ($\bar{\nu}$) in the final states of the decays cannot be directly detected, but are treated as missing energy (\cancel{E}) in experiments. So far most experiments can only obtain the upper limits on the decay branching ratios associated with $\nu\bar{\nu}$ [11–21].

The experimental searches have given the strictest constraints on kaon FCNC decays. Recently, the upper bound on $K_L \rightarrow \pi^0\bar{\nu}\nu$ from the KOTO experiment at J-PARC [11] has been given to be $\mathcal{B}(K_L \rightarrow \pi^0\bar{\nu}\nu)_{\text{KOTO}} < 3.0 \times 10^{-9}$ at 90% confidence level (C.L.), which is slightly greater than the SM prediction of $\mathcal{B}(K_L \rightarrow \pi^0\bar{\nu}\nu)_{\text{SM}} = (3.4 \pm 0.6) \times 10^{-11}$ [22]. On the other hand, the decay of $K^+ \rightarrow \pi^+\bar{\nu}\nu$ has been measured, namely, $\mathcal{B}(K^+ \rightarrow \pi^+\bar{\nu}\nu)_{\text{NA62}} = (11.0^{+4.0}_{-3.5}(\text{stat}) \pm 0.3(\text{syst})) \times 10^{-11}$ at 68% C.L. from the NA62 experiment at CERN [12] and $\mathcal{B}(K^+ \rightarrow \pi^+\bar{\nu}\nu)_{\text{E949}} = (17.3^{+11.5}_{-10.5}) \times 10^{-11}$ from the E949 experiment at BNL [13]. These results are consistent with the SM prediction of $\mathcal{B}(K^+ \rightarrow \pi^+\bar{\nu}\nu)_{\text{SM}} = (8.4 \pm 1.0) \times 10^{-11}$ [22] within one standard deviation. It is clear that the room for NP in $K \rightarrow \pi\cancel{E}$ has become quite small.

However, the searches for NP in the FCNC decay processes of charmed and bottomed hadrons would still be possible. For example, the charmed meson and hyperon decays associated with \cancel{E} have been analyzed in Ref. [23]. The invisible decays of bottomed mesons have attracted more attention experimentally. For example, the upper bounds of branching ratios of $B \rightarrow K^{(*)}$, π , ρ modes have been given by the CLEO [14], BarBar [15–18], Belle [19–21] and Belle II [24] collaborations. Particularly, the Belle II [25] collaboration has estimated that the sensitivity for the measurement of the branching ratios of $B^{0(+)} \rightarrow K^{(*)0(+)}\bar{\nu}\nu$ processes can be increased by 25 – 30% in the near future, when assuming that 5 ab^{-1} of data will be taken on the $\Upsilon(5S)$ resonance. In addition, the future e^+e^- colliders, such as the FCC-ee [26–28] experiment, have shown the ability of precise measurements of FCNC processes. The current measurements of the experimental bounds which are listed as the first column in Table I are cited from Refs. [18, 20, 21]. The SM predictions cited

from [29, 30] contains both short-distance and long-distance contributions. In Table I,

TABLE I. The branching ratios (\mathcal{B}) (in units of 10^{-6}) of B decays involving missing energy.

Experimental bound [18, 20, 21] ^a	SM prediction [29, 30]	Invisible particles bound
$\mathcal{B}(B^\pm \rightarrow K^\pm \cancel{E}) < 16$	$\mathcal{B}(B^\pm \rightarrow K^\pm \nu \bar{\nu}) = 4.73 \pm 0.56$	$\mathcal{B}(B^\pm \rightarrow K^\pm \chi \chi) < 11.8$
$\mathcal{B}(B^\pm \rightarrow \pi^\pm \cancel{E}) < 14$	$\mathcal{B}(B^\pm \rightarrow \pi^\pm \nu \bar{\nu}) = 8.12 \pm 0.01$	$\mathcal{B}(B^\pm \rightarrow \pi^\pm \chi \chi) < 5.89$
$\mathcal{B}(B^\pm \rightarrow K^{*\pm} \cancel{E}) < 40$	$\mathcal{B}(B^\pm \rightarrow K^{*\pm} \nu \bar{\nu}) = 8.93 \pm 1.07$	$\mathcal{B}(B^\pm \rightarrow K^{*\pm} \chi \chi) < 32.1$
$\mathcal{B}(B^\pm \rightarrow \rho^\pm \cancel{E}) < 30$	$\mathcal{B}(B^\pm \rightarrow \rho^\pm \nu \bar{\nu}) = 0.48 \pm 0.18$	$\mathcal{B}(B^\pm \rightarrow \rho^\pm \chi \chi) < 29.7$

^a These experimental bounds are adopted by PDG-live, which are not certainly the latest or strictest constraints.

the differences between the first and second columns indicate that there are some rooms for new invisible particles of χ (shown as the third column) emitted in such processes. In Refs. [31–40], the effects of the invisible particles with various spins in the FCNC and neutral meson annihilation processes have been explored. While most of these previous studies in the literature are focused on mesons. There have been no related researches on bottomed baryons up to now. In this paper, we generalize the experimental upper bounds from B mesons to the corresponding decay modes of bottomed baryons, namely, Λ_b and Ξ_b . These modes are accessible for the Belle II collaboration [25], which will be able to obtain more sensitive results in future projects. Clearly, in the near future the experiments on bottomed baryons would provide an interesting window to probe with invisible particles.

In this work, we consider the bottomed baryonic FCNC decays of $\mathbf{B}_b \rightarrow \mathbf{B}_n \chi \chi$, where $\mathbf{B}_{n(b)}$ are (bottomed) baryons and χ represent light invisible particles, which are assumed to be Majorana fermions. Phenomenologically, these new invisible fermions of χ can weakly interact with the SM fermions via a mediator, which can be a scalar [41], pseudoscalar [42], vector or axial-vector [43] particle. In our study, we will concentrate on a general model-independent approach to introduce the effective Lagrangian, which contains all possible currents involving the invisible fermions with the coupling constants extracted from the experiments.

The paper is organized as follows: In Sec. II, we obtain the SM expectations of $\mathbf{B}_b \rightarrow \mathbf{B}_n \bar{\nu} \nu$. In Sec. III, we first construct the effective Lagrangian, which describes the coupling between the quarks and light invisible fermions. We then present the numerical results of

the upper limits for the decay branching ratios of $\mathbf{B}_b \rightarrow \mathbf{B}_n \chi \chi$. The hadronic transition matrix elements are evaluated based on the QCD light-cone sum rules (LCSR) and modified bag model (MBM). Finally, we give the conclusion in Sec. IV.

II. THE SM EXPECTATIONS

The FCNC decay processes of bottomed baryons with missing energy are described in Fig. 1, where \mathbf{B}_b and \mathbf{B}_n represent the initial and final baryons, respectively; $q = b$ and $q_f = s(d)$ are initial and final quarks, respectively; and $q_{2(3)}$ are the spectator quarks.

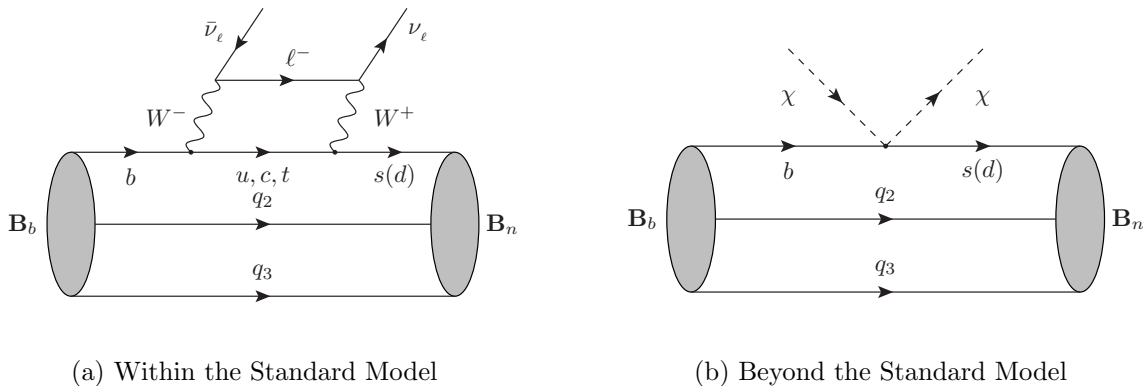


FIG. 1. Feynman diagrams of bottomed baryon FCNC decays with missing energy.

In the SM, there is no tree-level contribution to the FCNC decays of $\mathbf{B}_b \rightarrow \mathbf{B}_n \bar{\nu} \nu$. The first-order contributions to these processes come from the penguin and box diagrams as shown in Fig. 1a, which can be described by the effective Lagrangian, given by [44]

$$\mathcal{L}_{\bar{\nu}\nu} = \frac{4G_F}{\sqrt{2}} \frac{\alpha}{2\pi \sin^2 \theta_W} \sum_{\ell=e,\mu,\tau} \sum_{q=u,c,t} V_{bq} V_{sq} X^\ell(x_q) (\bar{s}_L \gamma^\mu b_L) (\bar{\nu}_{\ell L} \gamma_\mu \nu_{\ell L}), \quad (1)$$

with

$$X^\ell(x_q) = \frac{x_q}{8} \left[\frac{x_q + 2}{x_q - 1} + \frac{3(x_q - 2)}{(x_q - 1)^2} \ln x_q \right], \quad (2)$$

where G_F represents the Fermi coupling constant, α corresponds to the fine structure constant, θ_W stands for the Weinberg angle, V_{ij} are the Cabibbo–Kobayashi–Maskawa (CKM) matrix elements, and $x_q = m_q^2/M_W^2$ with m_q (M_W) being the mass of the quark (W -boson). Consequently, the transition amplitude is given by

$$\langle \mathbf{B}_n \bar{\nu} \nu | \mathcal{L}_{\bar{\nu}\nu} | \mathbf{B}_b \rangle = \frac{\sqrt{2} G_F \alpha}{4\pi \sin^2 \theta_W} V_{bt} V_{st} X^\ell(x_t) \langle \mathbf{B}_n | \bar{s} \gamma^\mu (1 - \gamma^5) b | \mathbf{B}_b \rangle \times \bar{u}_{\nu_\ell} \gamma_\mu (1 - \gamma^5) v_{\nu_\ell}. \quad (3)$$

The baryonic transition matrix elements can be parameterized by the form factors (FFs) of $f_i^{V,A}$ ($i = 1, 2, 3$), f^S and f^P , defined by

$$\begin{aligned}
\langle \mathbf{B}_n(P_f, s_f) | (\bar{q}_f \gamma_\mu q) | \mathbf{B}_b(P, s) \rangle &= \bar{u}_{\mathbf{B}_n}(P_f, s_f) \left[\gamma_\mu f_1^V(q^2) + i\sigma_{\mu\nu} \frac{q^\nu}{M} f_2^V(q^2) + \frac{q^\mu}{M} f_3^V(q^2) \right] u_{\mathbf{B}_b}(P, s), \\
\langle \mathbf{B}_n(P_f, s_f) | (\bar{q}_f q) | \mathbf{B}_b(P, s) \rangle &= \bar{u}_{\mathbf{B}_n}(P_f, s_f) f^S(q^2) u_{\mathbf{B}_b}(P, s), \\
\langle \mathbf{B}_n(P_f, s_f) | (\bar{q}_f \gamma_\mu \gamma^5 q) | \mathbf{B}_b(P, s) \rangle &= \bar{u}_{\mathbf{B}_n}(P_f, s_f) \left[\gamma_\mu f_1^A(q^2) + i\sigma_{\mu\nu} \frac{q^\nu}{M} f_2^A(q^2) + \frac{q^\mu}{M} f_3^A(q^2) \right] \gamma^5 u_{\mathbf{B}_b}(P, s), \\
\langle \mathbf{B}_n(P_f, s_f) | (\bar{q}_f \gamma^5 q) | \mathbf{B}_b(P, s) \rangle &= \bar{u}_{\mathbf{B}_n}(P_f, s_f) f^P(q^2) \gamma^5 u_{\mathbf{B}_b}(P, s),
\end{aligned} \tag{4}$$

where q corresponds to the momentum transfer, and M is the mass of the initial baryon. We will evaluate these elements in terms of the MBM, which works well for the heavy baryonic decays [45–49]. In the MBM, the baryon wave functions at rest are read as

$$\Psi(x_{q_1}, x_{q_2}, x_{q_3}) = \mathcal{N} \int d^3\vec{x} \prod_{i=1,2,3} \phi_{q_i}(\vec{x}_{q_i} - \vec{x}) e^{-iE_{q_i} t_{q_i}}, \tag{5}$$

where q_i are the quark components of the baryons, \mathcal{N} the overall normalization constant, x_{q_i} (E_{q_i}) the spacetime coordinates (energies) of q_i , and $\phi_{q_i}(x)$ the quark wave functions inside a static bag, located at the center, given by

$$\phi_q(\vec{x}) = \begin{pmatrix} \omega_q + j_0(p_q r) \chi_q \\ i\omega_q - j_1(p_q r) \hat{r} \cdot \vec{\sigma} \chi_q \end{pmatrix}. \tag{6}$$

Here, $j_{0,1}$ represent the spherical Bessel functions, $\omega_{q\pm} = \sqrt{T_q \pm M_q}$ with T_q the kinematic energies, and χ_q are the two component spinors. By demanding that quark currents shall not penetrate the boundary of bags, we have the boundary condition

$$\tan(p_q R) = \frac{p_q R}{1 - M_q R - E_q R}, \tag{7}$$

where R is the bag radius, resulting in that the magnitudes of 3-momenta are quantized, which can be analogous to the well-know infinite square well.

Several remarks are in order to address some of the issues in the bag model. One of the main theoretical inconsistencies is that the chiral symmetry is broken by the boundary even when the quarks are massless. It is due to that only the three-momenta are flipped when the quarks meet the boundary, whereas the spin directions are unchanged. Thus, the boundary inevitably alters the handedness of the quarks. The chiral symmetry plays an important role in the light quark system. Nonetheless, as we only consider the $b \rightarrow s$ transitions, of

which the chiral symmetry is already broken badly by the b quark mass, it shall not cause severe problems. On the other hand, the bag model originally describes a baryon state at rest. Therefore, the form factors at the maxima recoil point ($q_{max}^2 = (M_{\Lambda_b} - M_\Lambda)^2$) would be more reliable. In particular, the axial form factors of the $n \rightarrow p$ transition is found to be $f_1^A = 1.31$, which is very close to 1.27 from the experiments.

By sandwiching the operators, we arrive

$$\int \langle \Lambda | \bar{s} \Gamma b(x) e^{iqx} | \Lambda_b \rangle d^4x = \mathcal{Z} \int d^3\vec{x}_\Delta \Gamma_{sb}(\vec{x}_\Delta) \prod_{q_j=u,d} D_{q_j}(\vec{x}_\Delta), \quad (8)$$

with

$$\begin{aligned} \mathcal{Z} &\equiv (2\pi)^4 \delta^4(p_{\Lambda_b} - p_\Lambda - q) \mathcal{N}_{\Lambda_b} \mathcal{N}_\Lambda, \\ D_{q_j}(\vec{x}_\Delta) &\equiv \sqrt{1-v^2} \int d^3\vec{x} \phi_{q_j}^\dagger \left(\vec{x} + \frac{1}{2}\vec{x}_\Delta \right) \phi_{q_j} \left(\vec{x} - \frac{1}{2}\vec{x}_\Delta \right) e^{-2iE_{q_j}\vec{v}\cdot\vec{x}}, \\ \Gamma_{sb}(\vec{x}_\Delta) &= \int d^3\vec{x} \phi_s \left(\vec{x} + \frac{1}{2}\vec{x}_\Delta \right) \gamma^0 S_{-\vec{v}} \Gamma S_{-\vec{v}} \phi_b \left(\vec{x} - \frac{1}{2}\vec{x}_\Delta \right) e^{i(M_\Lambda + M_{\Lambda_b} - E_s - E_b)\vec{v}\cdot\vec{x}}, \end{aligned} \quad (9)$$

where Γ are arbitrary Dirac matrices, and $S_{\vec{v}}$ the Lorentz boost matrix of Dirac spinors. We have taken the initial (final) state as Λ_b (Λ) for an concrete example. To simplify the algebra, the Briet frame is chosen, where Λ_b and Λ have the velocity $-\vec{v}$ and \vec{v} , respectively. Notably, all the parameters of the model are extracted from the mass spectra, given as [50]

$$R = 4.8 \text{ GeV}^{-1}, \quad M_{u,d} = 0, \quad M_s = 0.28 \text{ GeV}, \quad M_b = 5.093 \text{ GeV}. \quad (10)$$

In general, the bag radius of Λ_b differs from the one of Λ . Nevertheless, in calculating the transition matrix elements, the different bag radii between the initial and final states lead to several theoretical difficulties. In this work, we take the bag radii of the initial and final baryons as the same and allow it to vary 5%, which shall cover the reasonable range. We consider the bottomed baryon decays of ($\Lambda_b \rightarrow \Lambda \bar{\nu} \nu$ and $\Xi_b^{0(-)} \rightarrow \Xi^{0(-)} \bar{\nu} \nu$) and ($\Lambda_b \rightarrow n \bar{\nu} \nu$, $\Xi_b^{0(-)} \rightarrow \Sigma^{0(-)} \bar{\nu} \nu$, and $\Xi_b^0 \rightarrow \Lambda \bar{\nu} \nu$), due to the ($b \rightarrow s$) and ($b \rightarrow d$) transitions at quark level, respectively. The FFs can be extracted straightforwardly after the computations, which are shown in Figs. 2-7 along with their q^2 dependencies, where the solid lines represent the central values, and the shadows between the dashed lines correspond to the errors estimated by varying the bag radius of $R = 4.8 \text{ GeV}^{-1}$ within $\pm 5\%$.

By integrating the three-body phase space, we obtain the decay branching ratio to be

$$\mathcal{B}(\mathbf{B}_b \rightarrow \mathbf{B}_n \bar{\nu} \nu) = \frac{1}{512\pi^3 M^3 \Gamma_{\mathbf{B}_b}} \int \frac{dq^2}{q^2} \lambda^{1/2}(M^2, q^2, M_f^2) \lambda^{1/2}(q^2, m_1^2, m_2^2) \int d\cos\theta \sum |\mathcal{M}|^2, \quad (11)$$

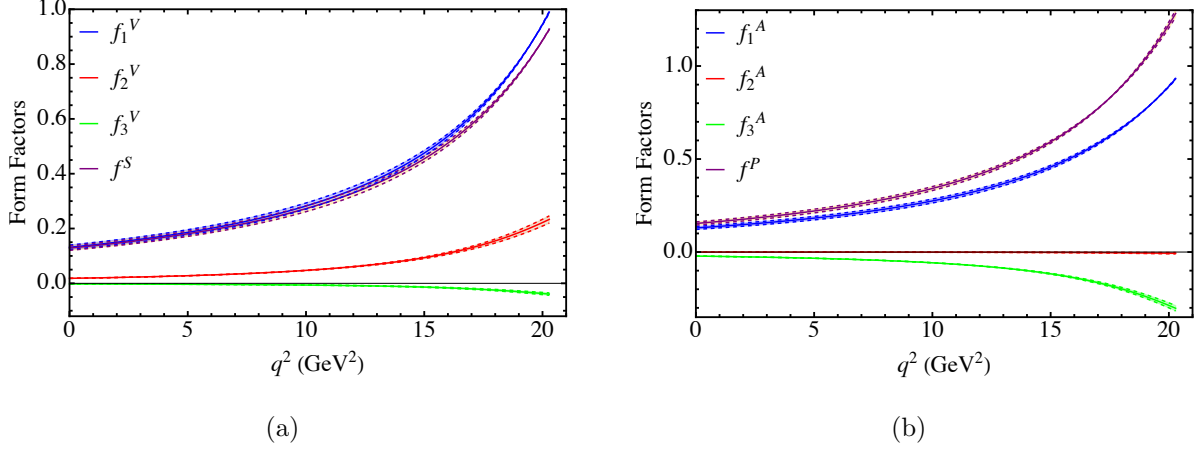


FIG. 2. Form factors of $\Lambda_b \rightarrow \Lambda$ as functions of q^2

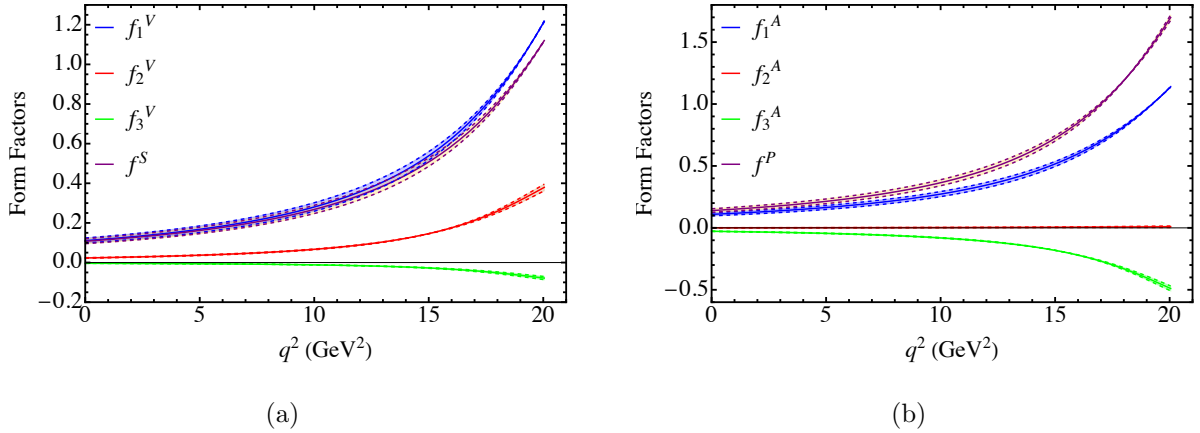


FIG. 3. Form factors of $\Xi_b^{0(-)} \rightarrow \Xi^{0(-)}$ as functions of q^2

where $\lambda(x, y, z) = x^2 + y^2 + z^2 - 2xy - 2xz - 2yz$ is the Källén function, M , M_f , m_1 and m_2 correspond to the masses of the initial baryon, final baryon, neutrino and anti-neutrino, respectively, θ is the phase space angle, $\Gamma_{\mathbf{B}_b}$ represents the total width of the initial baryon, and \mathcal{M} stands for the amplitude. As the three generations of neutrinos are indistinguishable experimentally, the final results need to be multiplied by three. For the $b \rightarrow s$ transition, the decay branching ratios associated with neutrino and anti-neutrino pairs are as follows:

$$\begin{aligned} \mathcal{B}(\Lambda_b \rightarrow \Lambda \bar{\nu} \nu) &= 5.52_{-0.28}^{+0.28} \times 10^{-6}, \\ \mathcal{B}(\Xi_b^{0(-)} \rightarrow \Xi^{0(-)} \bar{\nu} \nu) &= 7.80_{-0.67}^{+0.71} \times 10^{-6}. \end{aligned} \quad (12)$$

Here, due to the SU(3) flavor symmetry, the branching ratios of Ξ_b^0 and Ξ_b^- are considered approximately to be equal. The uncertainties of \mathcal{B} are about $\pm 5\%$ to $\pm 10\%$. Note that our results of $(\Lambda_b \rightarrow \Lambda \bar{\nu} \nu)$ in Eq. (12) is smaller than the previous prediction in Ref. [51].

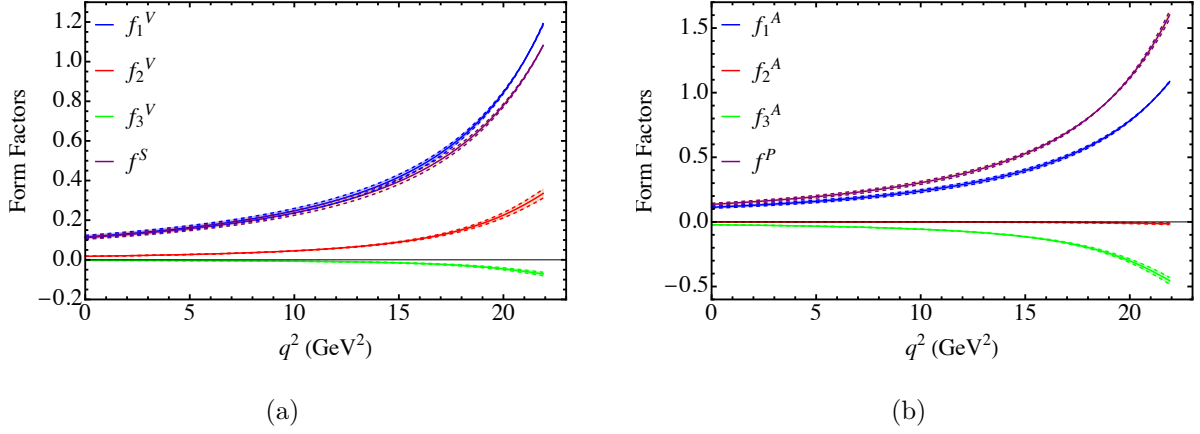


FIG. 4. Form factors of $\Lambda_b \rightarrow n$ as functions of q^2

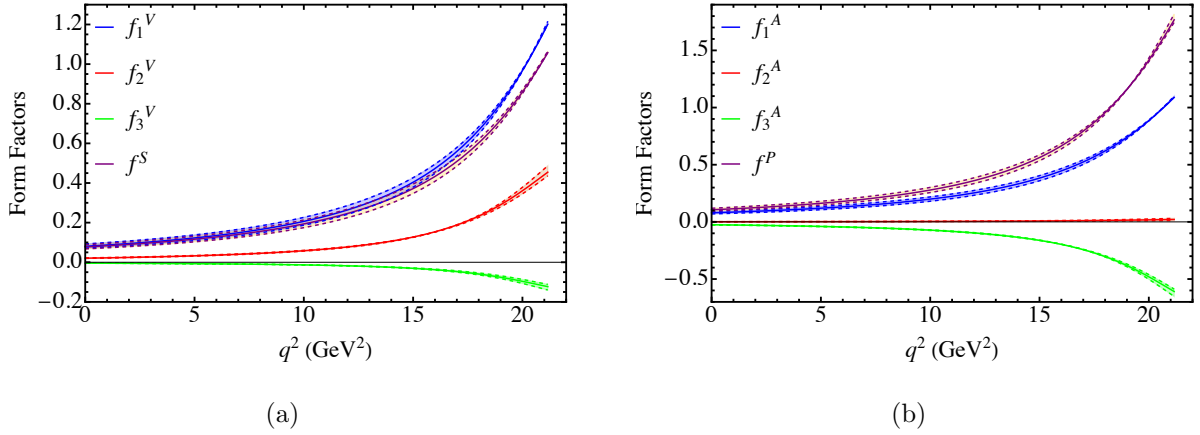


FIG. 5. Form factors of $\Xi_b^- \rightarrow \Sigma^-$ as functions of q^2

Similarly, for the $b \rightarrow d$ transition we have that

$$\begin{aligned}
 \mathcal{B}(\Lambda_b \rightarrow n \bar{\nu} \nu) &= 2.76_{-0.16}^{+0.17} \times 10^{-7}, \\
 \mathcal{B}(\Xi_b^- \rightarrow \Sigma^- \bar{\nu} \nu) &= 2.65_{-0.26}^{+0.29} \times 10^{-7}, \\
 \mathcal{B}(\Xi_b^0 \rightarrow \Sigma^0 \bar{\nu} \nu) &= 1.24_{-0.12}^{+0.13} \times 10^{-7}, \\
 \mathcal{B}(\Xi_b^0 \rightarrow \Lambda \bar{\nu} \nu) &= 3.88_{-0.40}^{+0.37} \times 10^{-8},
 \end{aligned} \tag{13}$$

which are about one to two orders of magnitude smaller than the modes in Eq. (12), due to the ratio of the Cabibbo–Kobayashi–Maskawa (CKM) matrix elements, $|V_{td}/V_{ts}| \sim \mathcal{O}(\lambda)$. As a result, the SM predictions of bottomed baryonic FCNC processes with \cancel{E} are $\mathcal{O}(10^{-8}) - \mathcal{O}(10^{-6})$. If the experimental detections of these decays are larger than the values in Eqs. (12)-(13), the new invisible neutral particles from NP are expected.

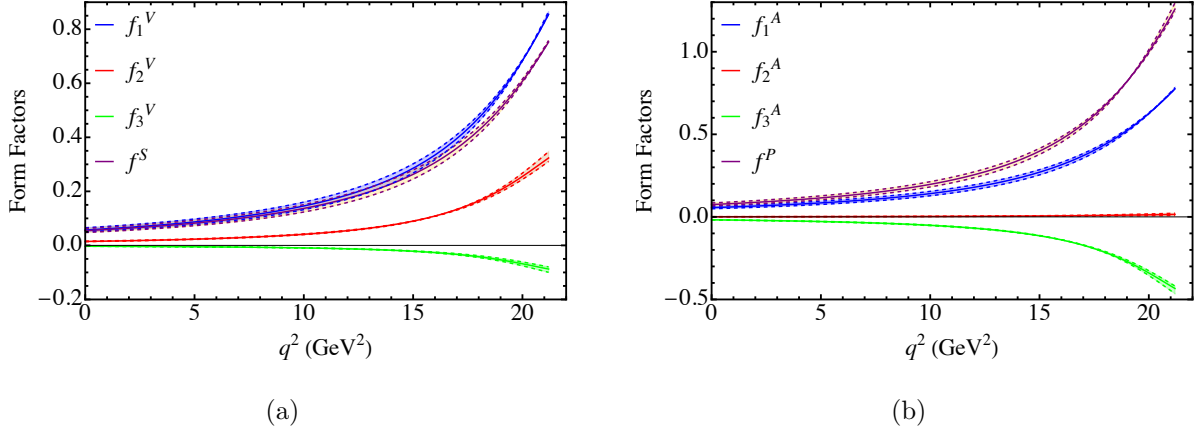


FIG. 6. Form factors of $\Xi_b^0 \rightarrow \Sigma^0$ as functions of q^2

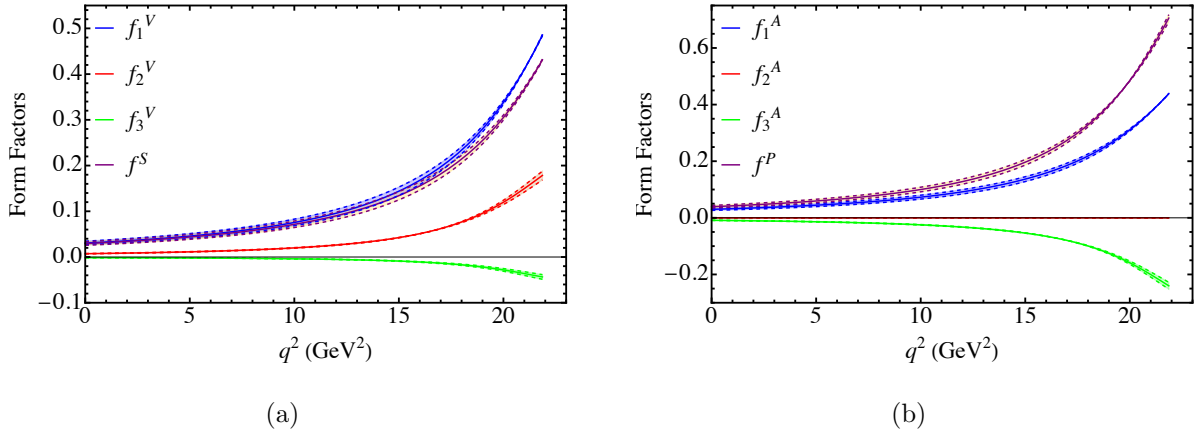


FIG. 7. Form factors of $\Xi_b^0 \rightarrow \Lambda$ as functions of q^2

III. PROCESSES WITH INVISIBLE PARTICLES

A. Effective Lagrangian

In Fig. 1b, two spin-1/2 invisible Majorana particles of $\chi\chi$ are assumed to be emitted in the process, in which the four-fermion vertex may be generated at tree or loop level by introducing new physical mediators in specific models [41–43]. Under the low energy scale, the model-independent effective Lagrangian is given by

$$\mathcal{L}_{eff} = \sum_{i=1}^6 g_{mi} Q_i, \quad (14)$$

where g_{fi} are the phenomenological coupling constants, which are taken at the new physical energy scale Λ . There are 6 independent dimension-six effective operators, which have the

forms:

$$\begin{aligned}
Q_1 &= (\bar{q}_f q)(\chi\chi), & Q_2 &= (\bar{q}_f \gamma^5 q)(\chi\chi), & Q_3 &= (\bar{q}_f q)(\chi\gamma^5\chi), \\
Q_4 &= (\bar{q}_f \gamma^5 q)(\chi\gamma^5\chi), & Q_5 &= (\bar{q}_f \gamma_\mu q)(\chi\gamma^\mu\gamma^5\chi), & Q_6 &= (\bar{q}_f \gamma_\mu \gamma^5 q)(\chi\gamma^\mu\gamma^5\chi),
\end{aligned} \tag{15}$$

where the invisible particles of χ have been assumed to be the Majorana type. Since $\chi\gamma^\mu\chi = 0$ and $\chi\sigma^{\mu\nu}\chi = 0$, there is no contribution from the vector or tensor current.

The upper limits of the coupling constants in the effective Lagrangian can be extracted from the differences between the theoretical predictions and experimental data of the B meson FCNC decays, such as $B^- \rightarrow K^-(K^{*-}) + \cancel{E}$ and $B^- \rightarrow \pi^-(\rho^-) + \cancel{E}$, of which Feynman diagram is illustrated as Fig. 8. For the $0^- \rightarrow 0^-$ meson decays of $M^- \rightarrow M_f^- \chi\chi$, only

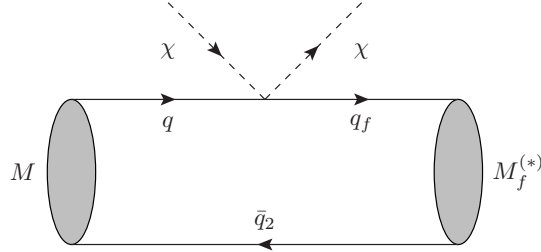


FIG. 8. Feynman diagram of bottomed meson FCNC decays with invisible particles.

operators $Q_{1,3,5}$ give the contributions. And for the $0^- \rightarrow 1^-$ meson decays of $M^- \rightarrow M_f^{*-} \chi\chi$ only operators $Q_{2,4,5,6}$ give the contributions. The amplitudes of the $0^- \rightarrow 0^-$ decays can be simplified as Eq. (16), and the amplitudes of the $0^- \rightarrow 1^-$ decays can be simplified as Eq. (17),

$$\begin{aligned}
\langle M_f^- \chi\chi | \mathcal{L}_{eff} | M^- \rangle &= 2g_{m1} \langle M_f^- | (\bar{q}_f q) | M^- \rangle \bar{u}_\chi v_\chi + 2g_{m3} \langle M_f^- | (\bar{q}_f q) | M^- \rangle \bar{u}_\chi \gamma^5 v_\chi \\
&+ 2g_{m5} \langle M_f^- | (\bar{q}_f \gamma_\mu q) | M^- \rangle \bar{u}_\chi \gamma^\mu \gamma^5 v_\chi,
\end{aligned} \tag{16}$$

$$\begin{aligned}
\langle M_f^{*-} \chi\chi | \mathcal{L}_{eff} | M^- \rangle &= 2g_{m2} \langle M_f^{*-} | (\bar{q}_f \gamma^5 q) | M^- \rangle \bar{u}_\chi v_\chi + 2g_{m4} \langle M_f^{*-} | (\bar{q}_f \gamma^5 q) | M^- \rangle \bar{u}_\chi \gamma^5 v_\chi \\
&+ 2g_{m5} \langle M_f^{*-} | (\bar{q}_f \gamma_\mu q) | M^- \rangle \bar{u}_\chi \gamma^\mu \gamma^5 v_\chi + 2g_{m6} \langle M_f^{*-} | (\bar{q}_f \gamma_\mu \gamma^5 q) | M^- \rangle \bar{u}_\chi \gamma^\mu \gamma^5 v_\chi.
\end{aligned} \tag{17}$$

The hadronic transition matrix elements can be expressed as

$$\begin{aligned}
\langle M_f^- | (\bar{q}_f q) | M^- \rangle &= \frac{M^2 - M_f^2}{m_q - m_{q_f}} f_0(q^2), \\
\langle M_f^- | (\bar{q}_f \gamma_\mu q) | M^- \rangle &= (P + P_f)_\mu f_+(q^2) + (P - P_f)_\mu \frac{M^2 - M_f^2}{q^2} [f_0(q^2) - f_+(q^2)], \\
\langle M_f^- | (\bar{q}_f \sigma_{\mu\nu} q) | M^- \rangle &= i [P_\mu (P - P_f)_\nu - P_\nu (P - P_f)_\mu] \frac{2}{M + M_f} f_T(q^2),
\end{aligned} \tag{18}$$

and

$$\begin{aligned}
\langle M_f^{*-} | (\bar{q}_f \gamma^5 q) | M^- \rangle &= -i [\epsilon \cdot (P - P_f)] \frac{2M_f}{m_q + m_{q_f}} A_0(q^2), \\
\langle M_f^{*-} | (\bar{q}_f \gamma_\mu \gamma^5 q) | M^- \rangle &= i \left\{ \epsilon_\mu (M + M_f) A_1(q^2) - (P + P_f)_\mu \frac{\epsilon \cdot (P - P_f)}{M + M_f} A_2(q^2) \right. \\
&\quad \left. - (P - P_f)_\mu [\epsilon \cdot (P - P_f)] \frac{2M_f}{q^2} [A_3(q^2) - A_0(q^2)] \right\}, \\
\langle M_f^{*-} | (\bar{q}_f \gamma_\mu q) | M^- \rangle &= \varepsilon_{\mu\nu\rho\sigma} \epsilon^\nu P^\rho (P - P_f)^\sigma \frac{2}{M + M_f} V(q^2),
\end{aligned} \tag{19}$$

where m_{q_f} are the quark masses, f_j ($j = 0, +, T$), A_k ($k = 0 - 3$) and V are the FFs, which are evaluated from the method of the LCSR [52–54], and ϵ is the polarization vector of the final meson with the convention of $\varepsilon^{0123} = 1$.

In our calculation, we assume that only one operator contributes to the process at a time. By integrating the three-body phase space given in Eq. (11), the upper limits of the coupling constants g_{mi} can be obtained from Table I, given by

$$\mathcal{B}(M \rightarrow M_f^{(*)} \not{E})_{\text{exp}} - \mathcal{B}(M \rightarrow M_f^{(*)} \bar{\nu} \nu)_{\text{SM}} \geq \mathcal{B}(M \rightarrow M_f^{(*)} \chi \chi)_{Q_i} = \frac{|g_{mi}|^2 \tilde{\Gamma}_{ii}}{\Gamma_{M_B}}, \tag{20}$$

where $i = 1 - 6$, the subscript Q_i indicates that this operator contributes at this time, $\tilde{\Gamma}_{ii}$ are independent of the coupling constants, and Γ_{M_B} is the total width of the initial B meson. Notably, the partial decay width should be divided by two since the Majorana fermion is identical to its antiparticle. The upper limits of $|g_{mi}|^2$ on $(bs\chi\chi)$ and $(bd\chi\chi)$ vertices are shown as functions of m_χ in Fig. 9 with m_χ is the mass of χ . One can see that when $m_\chi \rightarrow 0$,

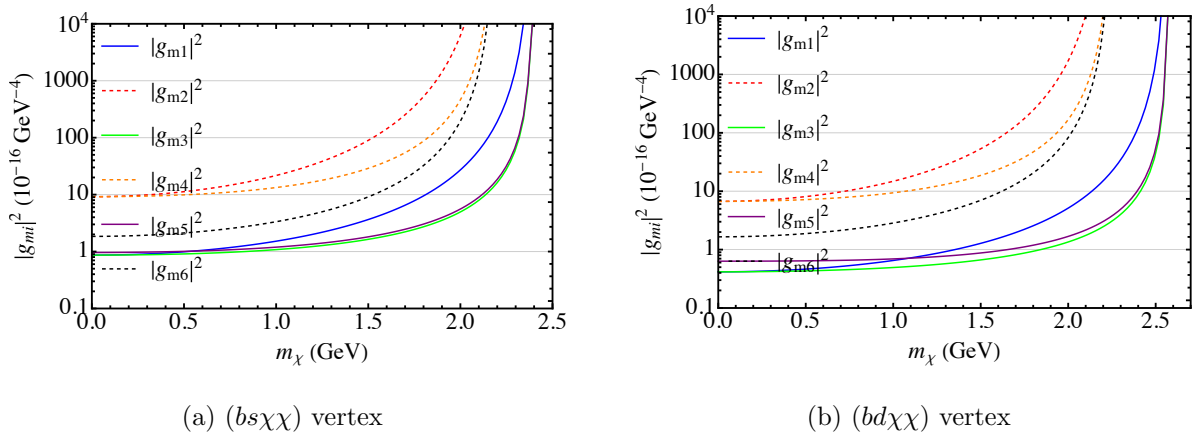


FIG. 9. Upper limits of $|g_{mi}|^2$ as functions of m_χ

the upper limits of $|g_{mi}|^2$ are $\mathcal{O}(10^{-17})$ to $\mathcal{O}(10^{-16})$. Note that the limits of $|g_{m2,4,6}|^2$ are

larger than these of $|g_{m1,3,5}|^2$, because the experimental upper bounds on the meson decay processes of $0^- \rightarrow 1^-$ are larger than those of $0^- \rightarrow 0^-$ given in Table I. When m_χ is larger, the bounds are getting looser as the phase space decreases.

B. Results with invisible particles

For the baryonic decays of $\mathbf{B}_b \rightarrow \mathbf{B}_n \chi \chi$, all operators in Eq. (15) should be considered. The decay amplitude can be expressed as

$$\begin{aligned} \langle \mathbf{B}_n \chi \chi | \mathcal{L}_{eff} | \mathbf{B}_b \rangle &= 2g_{m1} \langle \mathbf{B}_n | (\bar{q}_f q) | \mathbf{B}_b \rangle \bar{u}_\chi v_\chi + 2g_{m2} \langle \mathbf{B}_n | (\bar{q}_f \gamma^5 q) | \mathbf{B}_b \rangle \bar{u}_\chi v_\chi \\ &+ 2g_{m3} \langle \mathbf{B}_n | (\bar{q}_f q) | \mathbf{B}_b \rangle \bar{u}_\chi \gamma^5 v_\chi + 2g_{m4} \langle \mathbf{B}_n | (\bar{q}_f \gamma^5 q) | \mathbf{B}_b \rangle \bar{u}_\chi \gamma^5 v_\chi \\ &+ 2g_{m5} \langle \mathbf{B}_n | (\bar{q}_f \gamma_\mu q) | \mathbf{B}_b \rangle \bar{u}_\chi \gamma^\mu \gamma^5 v_\chi + 2g_{m6} \langle \mathbf{B}_n | (\bar{q}_f \gamma_\mu \gamma^5 q) | \mathbf{B}_b \rangle \bar{u}_\chi \gamma^\mu \gamma^5 v_\chi. \end{aligned} \quad (21)$$

Here, the baryonic transition matrix elements have been given by Eq. (4), while the numerical values of the FFs have been shown in Figs. 2-7. As above, we discuss the contribution of each operator separately. By integrating the three-body phase space in Eq. (11), $\tilde{\Gamma}_{ii}$ defined in Eq. (20) are obtained with the numerical results in Fig. 10. One can see that $\tilde{\Gamma}_{11,22,33,44,66}$ decrease to zero as m_χ increases due to the phase space reduction, while $\tilde{\Gamma}_{55}$ increases first and then decreases to zero. The upper bound of m_χ can be taken as $(M - M_f)/2$. When $m_\chi = 0$, we have that $\tilde{\Gamma}_{11} = \tilde{\Gamma}_{33}$ and $\tilde{\Gamma}_{22} = \tilde{\Gamma}_{44}$, since $\tilde{\Gamma}_{11,22}$ and $\tilde{\Gamma}_{33,44}$ are proportional to $(P_1 \cdot P_2 - m_\chi^2)$ and $(P_1 \cdot P_2 + m_\chi^2)$, respectively. The uncertainties of $\tilde{\Gamma}_{ii}$ are about $\pm 10\%$. It should be noted that $\tilde{\Gamma}_{ii}$ are independent of the coupling constants.

By combining $\tilde{\Gamma}_{ii}$ with the bounds of the coupling coefficients given in Fig. 9, we obtain the upper limits of the decay branching ratios associated with the SM predictions, as shown in Fig. 11. We see that in the most regions of m_χ , the upper limits of the branching ratios are $\mathcal{O}(10^{-6})$ to $\mathcal{O}(10^{-5})$, which are about of the same orders or an order of magnitude larger than the SM expectations of 10^{-8} to 10^{-6} . In Figs. 11c-11f, the solid pink lines representing the SM are close to the X axis. In particular, $Q_{2,4,6}$ make the dominant contributions. This is because the bounds on $|g_{m2,4,6}|^2$ are looser than these on $|g_{m1,3,5}|^2$. When $m_\chi \rightarrow (M - M_f)/2$, the upper limits for the branching ratios from $Q_{2,4,6}$ approach infinity, because the mass difference between the initial and final mesons is smaller than that between the initial and final baryons. For a larger value of m_χ , the baryon decays cannot be limited by the meson decay channels.

In Tables II, III and IV, we list the central values of upper limits of $\mathcal{B}(\mathbf{B}_b \rightarrow \mathbf{B}_n \chi \chi)$ for $m_\chi = 0, 1$ and 2 GeV, respectively. In Table II, we also show the SM predictions of

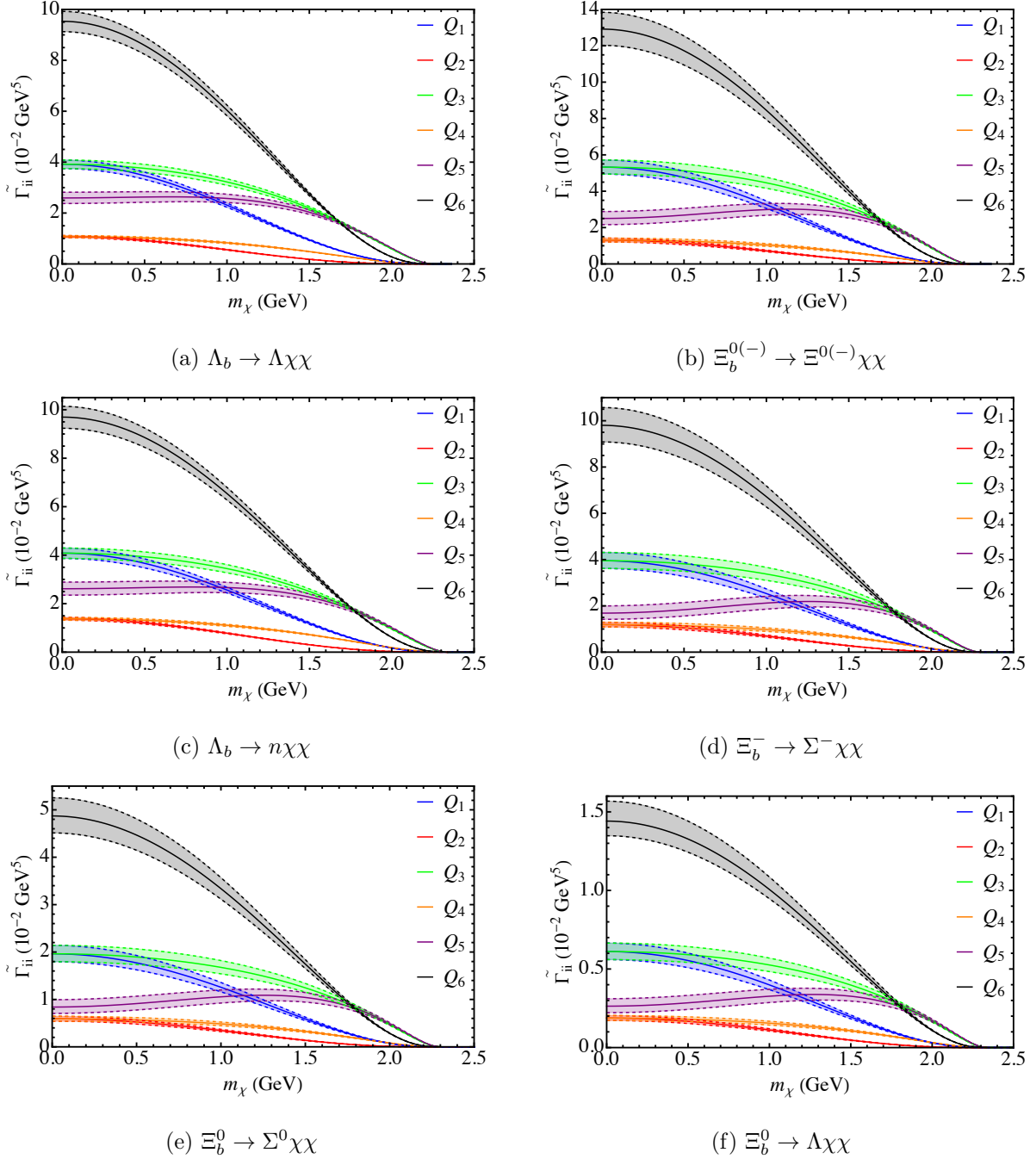


FIG. 10. $\tilde{\Gamma}_{ij}$ as functions of m_χ , where the shadows represent the errors estimated by varying the bag radius within $\pm 5\%$

$\mathcal{B}(\mathbf{B}_b \rightarrow \mathbf{B}_n \bar{\nu}\nu)$. We find that for the decays with $b \rightarrow s$ transition, the contributions from the new operators are almost of the same orders as the SM ones. While for these with $b \rightarrow d$ transition, the upper bounds of the decay modes with the invisible particles are about one to two orders of magnitude larger than $\mathcal{B}(\mathbf{B}_b \rightarrow \mathbf{B}_n \bar{\nu}\nu)$ due to the CKM matrix

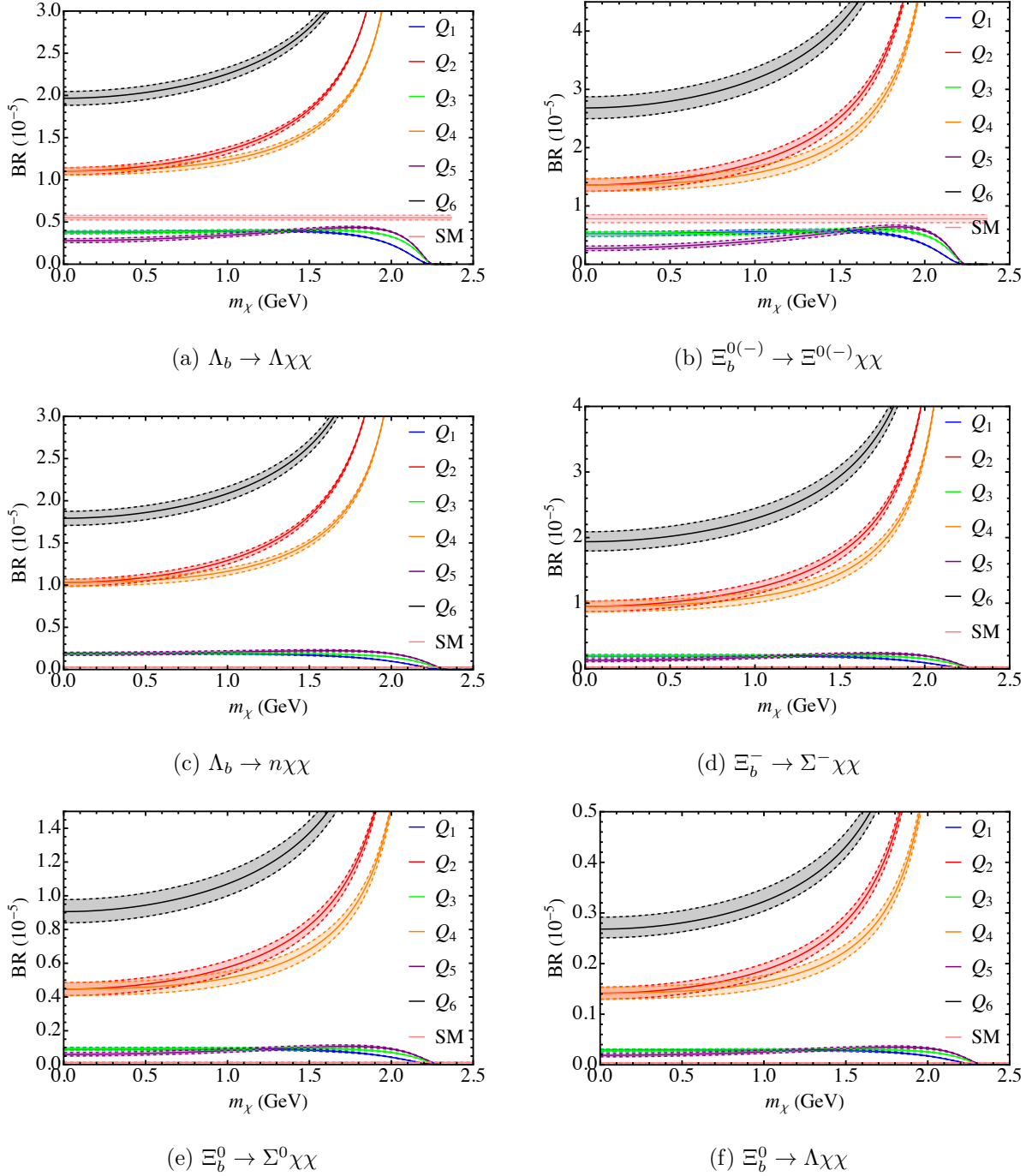


FIG. 11. Upper limits of $\mathcal{B}(\mathbf{B}_b \rightarrow \mathbf{B}_n \chi \chi)$ as functions of m_χ , where the shadows represent the errors estimated by varying the bag radius within $\pm 5\%$

element depressions. Clearly, it is more hopeful to distinguish new neutral particles from the SM neutrinos experimentally. When m_χ is larger, the upper limits of the contributions from $Q_{2,4,6}$ are getting looser. The upper limits of the branching ratios of decay modes with invisible particles are estimated to be $\mathcal{O}(10^{-5}) - \mathcal{O}(10^{-6})$. We expect that in the near

TABLE II. Upper limits of $\mathcal{B}(\mathbf{B}_b \rightarrow \mathbf{B}_n \chi \chi)$ when $m_\chi \rightarrow 0$ GeV (in units of 10^{-5})

Operator	$\Lambda_b \rightarrow \Lambda \chi \chi$	$\Xi_b^{0(-)} \rightarrow \Xi^{0(-)} \chi \chi$	$\Lambda_b \rightarrow n \chi \chi$	$\Xi_b^- \rightarrow \Sigma^- \chi \chi$	$\Xi_b^0 \rightarrow \Sigma^0 \chi \chi$	$\Xi_b^0 \rightarrow \Lambda \chi \chi$
Q_1	0.38	0.52	0.19	0.20	0.092	0.029
Q_2	1.1	1.4	1.0	0.95	0.45	0.14
Q_3	0.38	0.52	0.19	0.20	0.092	0.029
Q_4	1.1	1.4	1.0	0.95	0.45	0.14
Q_5	0.28	0.27	0.19	0.13	0.060	0.019
Q_6	2.0	2.7	1.8	1.9	0.91	0.27
SM	$\Lambda_b \rightarrow \Lambda \bar{\nu} \nu$	$\Xi_b^{0(-)} \rightarrow \Xi^{0(-)} \bar{\nu} \nu$	$\Lambda_b \rightarrow n \bar{\nu} \nu$	$\Xi_b^- \rightarrow \Sigma^- \bar{\nu} \nu$	$\Xi_b^0 \rightarrow \Sigma^0 \bar{\nu} \nu$	$\Xi_b^0 \rightarrow \Lambda \bar{\nu} \nu$
	0.55	0.78	0.028	0.027	0.012	0.0039

 TABLE III. Upper limits of $\mathcal{B}(\mathbf{B}_b \rightarrow \mathbf{B}_n \chi \chi)$ when $m_\chi = 1$ GeV (in units of 10^{-5})

Operator	$\Lambda_b \rightarrow \Lambda \chi \chi$	$\Xi_b^{0(-)} \rightarrow \Xi^{0(-)} \chi \chi$	$\Lambda_b \rightarrow n \chi \chi$	$\Xi_b^- \rightarrow \Sigma^- \chi \chi$	$\Xi_b^0 \rightarrow \Sigma^0 \chi \chi$	$\Xi_b^0 \rightarrow \Lambda \chi \chi$
Q_1	0.39	0.56	0.19	0.20	0.092	0.029
Q_2	1.4	1.8	1.3	1.2	0.58	0.19
Q_3	0.39	0.54	0.19	0.20	0.093	0.029
Q_4	1.2	1.6	1.2	1.1	0.51	0.16
Q_5	0.34	0.40	0.21	0.17	0.082	0.025
Q_6	2.3	3.2	2.1	2.3	1.1	0.32

future, experiments on the bottomed baryon FCNC decays could give more relevant results for comparisons.

IV. CONCLUSION

We have studied the light invisible Majorana fermions in the FCNC processes of the long-lived bottomed baryons. The model-independent effective Lagrangian which contains six operators has been introduced to describe the couplings between the quarks and invisible Majorana fermions. The bounds of the coupling constants have been extracted from

TABLE IV. Upper limits of $\mathcal{B}(\mathbf{B}_b \rightarrow \mathbf{B}_n \chi \chi)$ when $m_\chi = 2$ GeV (in units of 10^{-5})

Operator	$\Lambda_b \rightarrow \Lambda \chi \chi$	$\Xi_b^{0(-)} \rightarrow \Xi^{0(-)} \chi \chi$	$\Lambda_b \rightarrow n \chi \chi$	$\Xi_b^- \rightarrow \Sigma^- \chi \chi$	$\Xi_b^0 \rightarrow \Sigma^0 \chi \chi$	$\Xi_b^0 \rightarrow \Lambda \chi \chi$
Q_1	0.22	0.33	0.096	0.091	0.042	0.017
Q_2	5.3	7.3	5.2	4.4	2.0	0.93
Q_3	0.32	0.49	0.14	0.15	0.071	0.026
Q_4	3.6	5.4	3.6	3.3	1.6	0.61
Q_5	0.38	0.57	0.19	0.20	0.091	0.032
Q_6	6.3	9.2	5.7	5.8	2.7	1.0

the differences between the experimental upper limits and SM predictions of the relevant B meson FCNC decays. Based on these bounds, we have predicted the upper limits of $\mathcal{B}(\mathbf{B}_b \rightarrow \mathbf{B}_n \chi \chi)$. In particular, we have found that the decay branching ratios of $\Lambda_b \rightarrow \Lambda \chi \chi$, $\Xi_b^{0(-)} \rightarrow \Xi^{0(-)} \chi \chi$, $\Lambda_b \rightarrow n \chi \chi$, $\Xi_b^- \rightarrow \Sigma^- \chi \chi$, $\Xi_b^0 \rightarrow \Sigma^0 \chi \chi$, and $\Xi_b^0 \rightarrow \Lambda \chi \chi$ can be as large as $(2.0, 2.7, 1.8, 1.9, 0.91, 0.27) \times 10^{-5}$, $(2.3, 3.2, 2.1, 2.3, 1.1, 0.32) \times 10^{-5}$, and $(6.3, 9.2, 5.7, 5.8, 2.7, 1.0) \times 10^{-5}$ with $m_\chi = 0, 1$, and 2 GeV, respectively. We are looking forward to the future experiments, such as those at Belle II, to get more measurements on bottomed baryons to find signs of new particles.

V. ACKNOWLEDGMENTS

This work is supported in part by the National Key Research and Development Program of China under Grant No. 2020YFC2201501 and the National Natural Science Foundation of China (NSFC) under Grant No. 12147103.

-
- [1] G. Buchalla and A. J. Buras, *Nucl. Phys. B* **412**, 106 (1994).
 - [2] M. Misiak and J. Urban, *Phys. Lett. B* **451**, 161 (1999).
 - [3] L. Mott and W. Roberts, *Int. J. Mod. Phys. A* **27**, 1250016 (2012).
 - [4] A. Khodjamirian, T. Mannel, and Y. M. Wang, *JHEP* **02**, 010 (2013).
 - [5] M. Bordone, G. Isidori, and A. Pattori, *Eur. Phys. J. C* **76**, 440 (2016).

- [6] S. Anderson *et al.* (CLEO), *Phys. Rev. Lett.* **87**, 181803 (2001).
- [7] R. Aaij *et al.* (LHCb), *Phys. Lett. B* **724**, 203 (2013).
- [8] R. Aaij *et al.* (LHCb), *JHEP* **02**, 104 (2016).
- [9] R. Aaij *et al.* (LHCb), *JHEP* **07**, 020 (2018).
- [10] S. Choudhury *et al.* (BELLE), *JHEP* **03**, 105 (2021).
- [11] J. K. Ahn *et al.* (KOTO), *Phys. Rev. Lett.* **122**, 021802 (2019).
- [12] R. Fiorenza *et al.* (NA62), *PoS NuFact2021*, 176 (2022).
- [13] A. V. Artamonov *et al.* (E949), *Phys. Rev. Lett.* **101**, 191802 (2008).
- [14] T. E. Browder *et al.* (CLEO), *Phys. Rev. Lett.* **86**, 2950 (2001).
- [15] B. Aubert *et al.* (BaBar), *Phys. Rev. Lett.* **94**, 101801 (2005).
- [16] B. Aubert *et al.* (BaBar), *Phys. Rev. D* **78**, 072007 (2008).
- [17] P. del Amo Sanchez *et al.* (BaBar), *Phys. Rev. D* **82**, 112002 (2010).
- [18] J. P. Lees *et al.* (BaBar), *Phys. Rev. D* **87**, 112005 (2013).
- [19] K. F. Chen *et al.* (Belle), *Phys. Rev. Lett.* **99**, 221802 (2007).
- [20] O. Lutz *et al.* (Belle), *Phys. Rev. D* **87**, 111103 (2013).
- [21] J. Grygier *et al.* (Belle), *Phys. Rev. D* **96**, 091101 (2017).
- [22] A. J. Buras, D. Buttazzo, J. Girschbacher, and R. Knegjens, *JHEP* **11**, 033 (2015).
- [23] G. Faisel, J. Y. Su, and J. Tandean, *JHEP* **04**, 246 (2021).
- [24] F. Abudinén *et al.* (Belle-II), *Phys. Rev. Lett.* **127**, 181802 (2021).
- [25] W. Altmannshofer *et al.* (Belle-II), *PTEP* **2019**, 123C01 (2019).
- [26] A. Abada *et al.* (FCC), *Eur. Phys. J. C* **79**, 474 (2019).
- [27] A. Abada *et al.* (FCC), *Eur. Phys. J. ST* **228**, 261 (2019).
- [28] A. Blondel, E. Graverini, N. Serra, and M. Shaposhnikov (FCC-ee study Team), *Nucl. Part. Phys. Proc.* **273-275**, 1883 (2016).
- [29] R. Bause, H. Gisbert, M. Golz, and G. Hiller, *JHEP* **12**, 061 (2021).
- [30] D. Du, A. X. El-Khadra, S. Gottlieb, A. S. Kronfeld, J. Laiho, E. Lunghi, R. S. Van de Water, and R. Zhou, *Phys. Rev. D* **93**, 034005 (2016).
- [31] C. Bird, P. Jackson, R. V. Kowalewski, and M. Pospelov, *Phys. Rev. Lett.* **93**, 201803 (2004).
- [32] C. Bird, R. V. Kowalewski, and M. Pospelov, *Mod. Phys. Lett.* **A21**, 457 (2006).
- [33] A. Badin and A. A. Petrov, *Phys. Rev. D* **82**, 034005 (2010).
- [34] J. F. Kamenik and C. Smith, *JHEP* **03**, 090 (2012).

- [35] S. N. Gninenko and N. V. Krasnikov, *Phys. Rev.* **D92**, 034009 (2015).
- [36] E. Bertuzzo, C. J. Caniu Barros, and G. Grilli di Cortona, *JHEP* **09**, 116 (2017).
- [37] D. Barducci, M. Fabbrichesi, and E. Gabrielli, *Phys. Rev.* **D98**, 035049 (2018).
- [38] G. Li, T. H. Wang, Y. Jiang, X. Z. Tan, and G. L. Wang, *JHEP* **03**, 028 (2019).
- [39] G. Li, T. H. Wang, Y. Jiang, J. B. Zhang, and G. L. Wang, *Phys. Rev. D* **102**, 095019 (2020).
- [40] G. Li, T. H. Wang, J. B. Zhang, and G. L. Wang, *Eur. Phys. J. C* **81**, 564 (2021).
- [41] S. Matsumoto, Y. L. S. Tsai, and P. Y. Tseng, *JHEP* **07**, 050 (2019).
- [42] K. C. Yang, *Phys. Rev.* **D94**, 035028 (2016).
- [43] M. Chala, F. Kahlhoefer, M. McCullough, G. Nardini, and K. Schmidt-Hoberg, *JHEP* **07**, 089 (2015).
- [44] T. Inami and C. S. Lim, *Prog. Theor. Phys.* **65**, 297 (1981).
- [45] C. Q. Geng, C. W. Liu, and T. H. Tsai, *Phys. Rev. D* **102**, 034033 (2020).
- [46] C. Q. Geng and C. W. Liu, *JHEP* **11**, 104 (2021).
- [47] C. W. Liu and C. Q. Geng, *JHEP* **01**, 128 (2022).
- [48] C. W. Liu and B. D. Wan, *Phys. Rev. D* **105**, 114015 (2022).
- [49] C. W. Liu and C. Q. Geng, [arXiv:2205.08158](https://arxiv.org/abs/2205.08158) [hep-ph].
- [50] W. X. Zhang, H. Xu, and D. Jia, *Phys. Rev. D* **104**, 114011 (2021).
- [51] C. H. Chen and C. Q. Geng, *Phys. Rev. D* **63**, 054005 (2001).
- [52] P. Ball and R. Zwicky, *Phys. Rev.* **D71**, 014015 (2005).
- [53] T. M. Aliev, M. Savci, and K. C. Yang, *Phys. Lett.* **B700**, 55 (2011).
- [54] A. Bharucha, D. M. Straub, and R. Zwicky, *JHEP* **08**, 098 (2016).